(Received 30 October 2023, Accepted 25 March 2024, Scheduled 3 April 2024)

Ultra Thin Highly Sensitive Metamaterial Absorber Based Refractive Index Sensor for Detecting Adulterants in Alcohol

Sagnik Banerjee[1], Ishani Ghosh[2], Mazed Billah Fahad[1], Santosh Kumar Mishra[3], Rahul Yadav[4], and Bhargav Appasani[3,*]

[1]*Department of Information Engineering, Electronics and Telecommunications, Sapienza University of Rome, Roma, Italy*
[2]*Department of Mechanical and Aerospace Engineering, Sapienza University of Rome, Roma, Italy*
[3]*School of Electronics Engineering, Kalinga Institute of Industrial Technology, Bhubaneswar, India*
[4]*Nokia Solutions and Networks Oy, Finland*

ABSTRACT: This research provides a unique design of a terahertz-frequency metamaterial absorber. The absorber shows resonance at frequency 5.01 THz where the peak absorption is 99.5%. A staggering quality factor of 125.25 is also discovered. Since the radiation is non-ionizing, the metamaterial absorber can function as a refractive index sensor and can be used for sensing applications. To support the chosen design parameter values, parametric analysis was performed. The resonance mechanism has been clearly explained using the surface current distribution plot, and the metamaterial nature of the sensor has also been justified using the impedance plot, followed by the plot showing the permeability and permittivity at the resonance frequency. By detecting changes in the refractive index of the surrounding medium, the proposed sensor finds application in detecting the percentage of water and percentage of methanol in alcohol solution. Methanol and water are two prominent contaminants of alcohol. It can detect the percentage of water in alcohol with a sensitivity of 2.105 THz/RIU and can detect percentage of methanol in alcohol with a sensitivity of 1.999 THz/RIU. This work can inspire future research on using THz metamaterial absorbers for quality assessment of food products and beverages.

1. INTRODUCTION

Metamaterials are composite structures created specifically to exhibit unusual characteristics including optical magnetism, negative permittivity, and negative refractive index [1]. Its capacity to absorb incoming electromagnetic radiation is one of its related qualities. This design of metamaterial absorbers has gained popularity in the research field due to its diverse application in various frequency bands [2]. Terahertz metamaterial absorbers (TMAs) are what they are known as when they operate in the terahertz frequency range [3]. A TMA's absorption peaks may be adjusted by altering its material properties, after which it can be applied to a variety of sensing tasks. In [4–6], terahertz sensing with metamaterial absorbers has been experimentally proven for determining the analyte thickness. The TMAs are utilized to create temperature sensors whose absorption peaks are sensitive to variations in the surrounding medium's temperature [7]. TMAs are frequently employed to determine the environment's refractive index.

A TMA-based refractive index sensor with 1450 GHz/RIU, with concentric square and circular gold rings has been presented in [8]. A gas sensor concept with a combined hexagonal ring resonator that operates at 1600 GHz/RIU has been put forth [9]. An inverted bracket-shaped refractive index sensor is proposed in [10] with 593.04. In this proposed design, a better Q factor is obtained, but the sensitivity being 1557 GHz/RIU is lowered and is also unable to detect alcohol percentage. To operate in the refractive index range of 1.0 to 1.60, a folded split-ring metamaterial graphene resonator with an extremely high sensitivity of 851000 GHz/RIU is developed [11]. Here, a very high sensitivity is obtained, but the quality factor has suffered. A dual-band TMA is designed in [12] with 1121 GHz/RIU. This design has a quality factor of 151.69 with its peak absorption at 99.068%. This is based on a combined hexagonal ring resonator on a GaAs substrate. The design parameters of various TMAs are summarized in Table 1. Lower sensitivity and drop in the absorption rate have been recently an issue for terahertz TMA-based sensors. From the above literature review, we can easily figure out that there is an urge to have such a design as well as a higher sensitivity. This paper's novel use is the ability to detect alcohol amounts using a terahertz metamaterial absorber.

Terahertz radiation can be sometimes referred to as T-rays, T-lights, or T-waves [13]. The terahertz region encompasses frequencies 0.1–10 THz and wavelengths 3 mm to 30 µm. Here, $1\,\text{THz} = 1\,\text{ps} = 33\,\text{cm}^{-1} = 0.3\,\text{mm} = 4.1\,\text{meV} = 48\,\text{K}$ [14]. The terahertz gap is a frequency range in the THz region where there are no feasible technologies for producing or detecting radiation. The importance of overcoming the gap has been discovered through the realization of THz frequency as a spectrum of molecular vibrations, such as crystalline photon, molecular rotational, as well as inter- and intra-molecular vibrations [15]. THz radiations include spectrum attributes such as non-invasive, non-ionizing, spectral fingerprinting, polar substance phase sensitivity, a good resolution of less than 1 mm, penetration capabilities, and coherent detection properties that

* Corresponding author: Bhargav Appasani (bhargav.appasanifet@kiit.ac.in).

TABLE 1. Comparison of various TMA-based sensors.

Ref No.	Quality Factor (Q-Factor)	Sensitivity (GHz/RIU)	Absorption Rate	Figure of Merit (FoM)	Range of Refractive Index	Step Size (RIU)	Alcohol Percentage Detection
[18]	44.00	1500	99.50%	25.000	1.34–1.39	0.005	No
[19]	92.75	1447	92.75%	36.175	1.30–1.40	0.005	No
[20]	22.05	300	99.00%	02.940	1.30–1.39	0.010	No
[21]	44.17	126	99.00%	10.500	1.00–1.20	0.200	No
[22]	40.10	834	99.50%	11.750	1.00–1.80	0.100	No
[23]	78.90	0.3537	90.00%	11.053	1.00–3.1622	0.500	No
[24]	24.73	2137	99.50%	5.36	1.00–1.60	1.100	No
[25]	481.08	1450	99.9%	301.45	1.00–1.05	0.0100	No
[26]	179.95	2372	99.80%	64.62	1.00–1.50	0.100	No
This paper	125.25	2105	99.50%	52.63	1.33–1.36	0.010	Yes

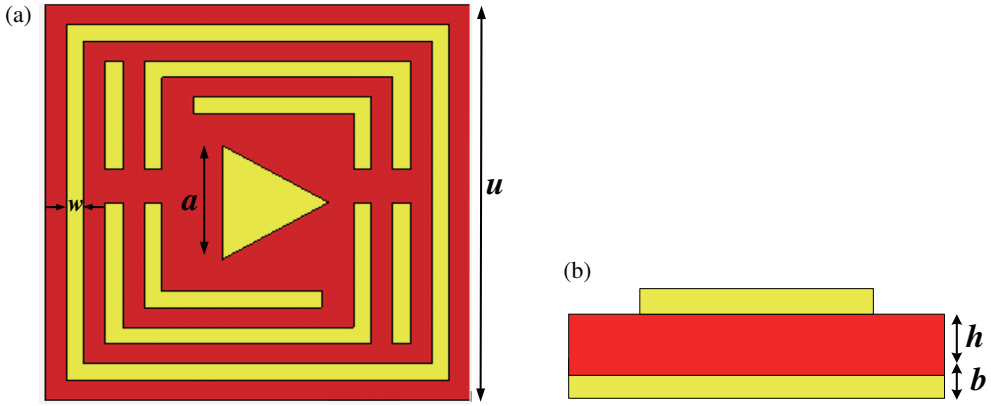

FIGURE 1. (a) Front view of the proposed structure and (b) side view of the proposed structure.

make the technique appealing for spectroscopy [16]. Being non-ionizing indicates that the radiation does not ionize the biomolecules in the tissue of interest [17], and no major tissue damage occurs. THz waves' phase sensitivity to polar substances, such as bodily fluids and water, gives higher contrast and absorption than X-rays [13].

Alcoholic drinks have complex structures that are widely produced and consumed in many nations around the sector. These drinks are normally composed of an ethanol and water mixture with really low amounts of other components such as acids, mineral salts, sugars, and a variety of others. Due to the increase in unemployment, alcoholic drinks may be pricey, encouraging individuals to ask for affordable alcohol. Methanol and ethanol have similar physical and chemical properties. To produce alcohol at a cheaper rate, a few non-institutional unlawful traders use methanol to increase the quantity of alcohol, and in this way, the charge of alcohol decreases consequently. Ingestion of these illegal alcoholic drinks that contain a high amount of methanol causes danger for humans. Methanol intake is accountable for forming formaldehyde and formic acid which causes serious health issues such as blindness, fatigue, and even demise. Many countries have confronted extensive health issues in their population correlated to alcohol contamination with methanol. The proposed sensor will detect the percentage of water and methanol in alcohol solution, thereby assessing the quality. To the best knowledge of the authors, existing works on THz metamaterials, as summarized in Table 1, have not attempted to detect water and methanol contamination in alcohol solution. This is the unique contribution of this work.

The remaining sections are arranged as follows. Section 2 discusses methods. Section 3 presents results and discussion. Section 4 closes the essay and offers suggestions for other study areas.

2. METHODOLOGY

Figure 1 shows the structural architecture of the proposed sensor. Gold covers the bottom and top surfaces and has a very outstanding conductivity of $4 \times 107\,\mathrm{Sm}^{-1}$. Gold was chosen as the metal patch because of its reflecting and low-loss characteristics. Gallium arsenide (GaAs), which has a thickness of $h = 6\,\mu\mathrm{m}$, makes up the sandwich layer that sits in between these two layers and functions as a dielectric spacer. The design's mechanical flexibility in the terahertz regime may even

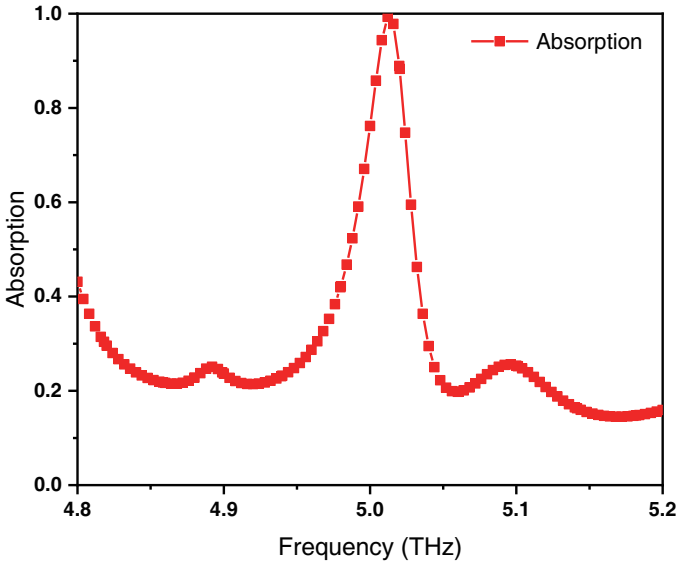

FIGURE 2. The proposed structure's absorption spectra.

be bent and employed for wearables based on metamaterials when the thickness 'h' is valued at a suitably low level. The ground metal plane is constructed to effectively prevent the passage of EM waves. Due to its fast electron mobility, GaAs is a compound semiconductor that is ideal for high-frequency applications and direct bandgap, which makes absorption of light more efficient, and there is a near-insulating zone for the sensor. The loss tangent of GaAs is 0.006, and its relative permittivity is 12.94. Furthermore, Gallium Arsenide possesses a wide band gap and very high resistivity, which makes it an ideal choice for a dielectric spacer. The bottom plane, which is constructed of gold, is $b = 2$ µm thick, and the suggested square unit cell has a length of 120 µm. A Triangular Patch Resonator (TPR) is present in the middle, with the distance from the triangle's center to each vertex being $a = 10$ µm, so it is an equilateral TPR. An array of Strip Resonator (SR) is present surrounding the TPR followed by an outer square ring with a width of $w = 4$ µm along with the SR.

Drude's model of metals provides a way to characterize the optical properties of noble metals such as gold using a complex permittivity plot having real and imaginary parts [27]:

$$\varepsilon_s(\omega) = \varepsilon_h - \frac{\omega_m^2}{\omega^2 + j\omega\gamma} \tag{1}$$

where ω represents the operating frequency in rad/s; ε_h represents the high-frequency permittivity (which is 12.94); m represents the plasma frequency; and γ represents the damping constant.

CST Microwave Studio is used to create the proposed structure and its accompanying simulations. CST Microwave Studio solves Maxwell's Equations in the frequency domain using the Finite Element Method. This solution generates a discrete frequency response with consistent steps over the bandwidth. When testing electrically smaller structures, the frequency domain solver is incredibly useful for getting electromagnetic wave responses in any material at any frequency value. S parameters are used to determine the frequency domain solver, and the calculation process ceases upon completion of the simulations. Although this process may take some time, results obtained from this method are often far more accurate than other methods. To ensure the accuracy of the results, Periodic Boundary Conditions are enforced on each side of the unit cell, and EM waves traveling along the negative z-axis are considered to impact upon the top surface of the suggested sensor.

To calculate the structure's absorption, the reflection and transmission of the incident plane wave must be removed. The absorbance for an effective terahertz MA is given by [28]:

$$A_s = 1 - T_s - R_s \tag{2}$$

where A_s, T_s, and R_s are the absorption, transmission, and reflection coefficients, respectively. Because EM wave transmission is inhibited, Eq. (2) shows that the reflection coefficient should be low to optimize absorption. Figure 2 shows that at 5.01 THz, near-perfect absorption of 99.5% is observed, and the full-width half-maximum (FWHM) is calculated to be 0.04 THz, indicating the narrow absorption bandwidth necessary for sensing applications. A sensor's quality factor (Q-factor) is a critical indication for any sensing application. It is the ratio of the resonant frequency to the FWHM and is presented in the following equation:

$$Q = \frac{Resonant\ frequency\ (f)}{Full\ Width\ Half\ Maximum\ (FWHM)} \tag{3}$$

The suggested design's Q-factor is determined using Eq. (3), and it is 125.25. It is an important parameter for proving the sensor's performance, and an elevated value is always preferred.

3. RESULTS AND DISCUSSIONS

From the impedance plot shown in Figure 3, we see that the real part is close to the free space impedance (377 Ω) at resonance.

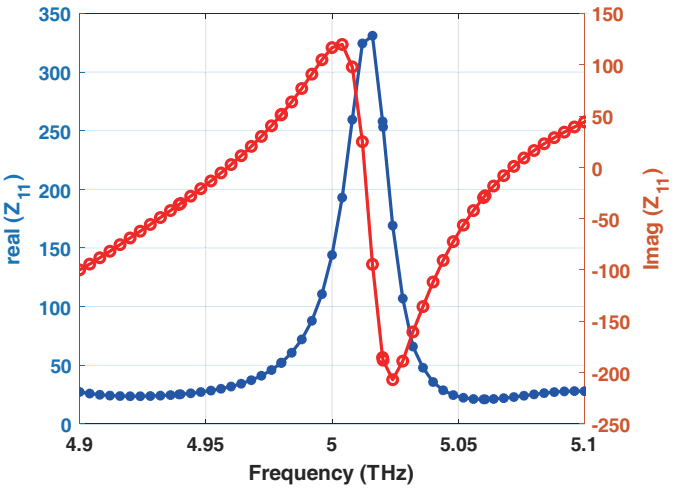

FIGURE 3. Impedance plot.

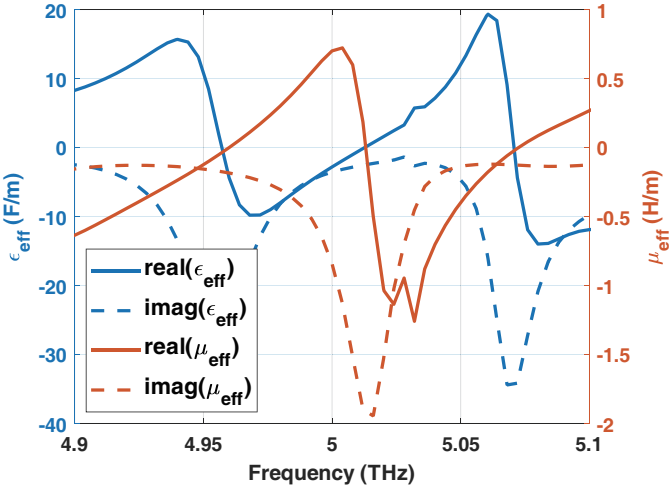

FIGURE 4. Effective Permittivity and permeability plot.

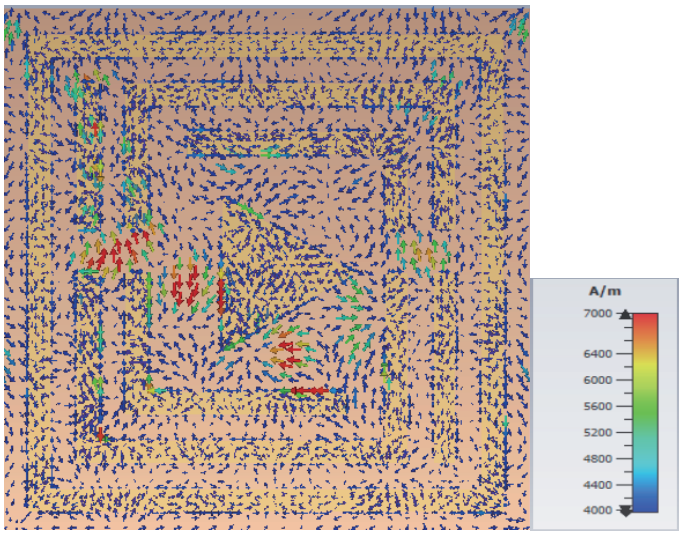

FIGURE 5. Surface current distribution plot.

The imaginary part is zero at resonance, so we say that we have impedance matching at resonance. Thereafter, the imaginary part becomes negative to positive which indicates that the reactance is capacitive to inductive. The input impedance at resonance frequency is $340-j201\,\Omega$, and its magnitude is $394.97\,\Omega$, which is near $377\,\Omega$ in free space.

Next, from the effective permittivity and permeability plot shown in Figure 4, we see that the real portion of the permittivity is slightly positive, and the real portion of permeability is negative at resonance. We can say that the designed metamaterial is a Mu-Negative Material (MNG), so we have absorption due to magnetic resonance. Had it been an Epsilon-Negative Material (ENG), then the absorption would have been due to plasmonic resonance. We can obtain the effective permeability, effective permittivity, and input impedance from the s-parameters using the following equations [29]:

$$Z_{11}(f) = \sqrt{\frac{(1+E_{11}(f))^2 - E_{21}^2(f)}{(1-E_{11}(f))^2 - E_{21}^2(f)}} \tag{4}$$

$$\varepsilon_{eff}(f) = \frac{c}{j\pi f d}\left(\frac{1-E_{21}-E_{11}}{1+E_{21}+E_{11}}\right) \tag{5}$$

$$\mu_{eff}(f) = \frac{c}{j\pi f d}\left(\frac{1-E_{21}+E_{11}}{1+E_{21}-E_{11}}\right) \tag{6}$$

From the surface current distribution plot shown in Figure 5, it is clear that the the currents circulate in small loops throughout the surface, and their concentration is maximum near the gaps of the inner resonators. This results in magnetic resonance. Similar results have been obtained from the effective permittivity and permeability plot as well which justifies the correctness of the obtained results. The induced current is the outer closed loop that is seen to have the same phase and run parallel to each other. A magnetic behavior caused by the presence of localized surface plasmon (LSP) is seen which produces coupling. At the metal-dielectric interface, LSPs are charged oscillations. Narrow absorption peaks at resonance are produced by magnetic coupling, which also minimizes the metallic absorption loss.

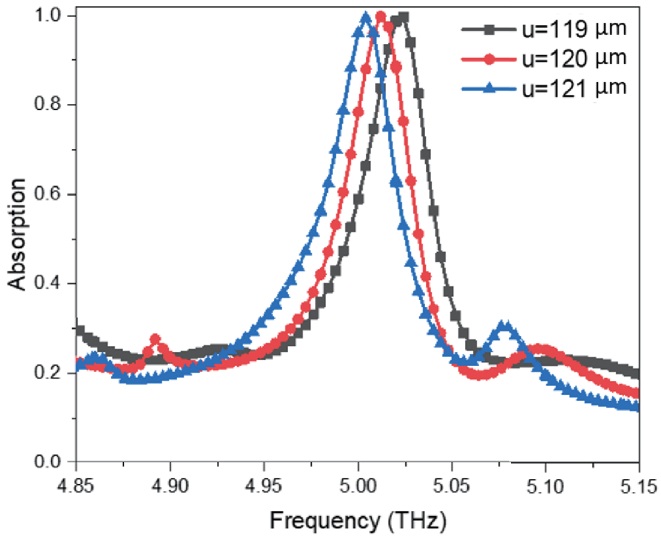

FIGURE 6. Parametric analysis of unit cell dimensions.

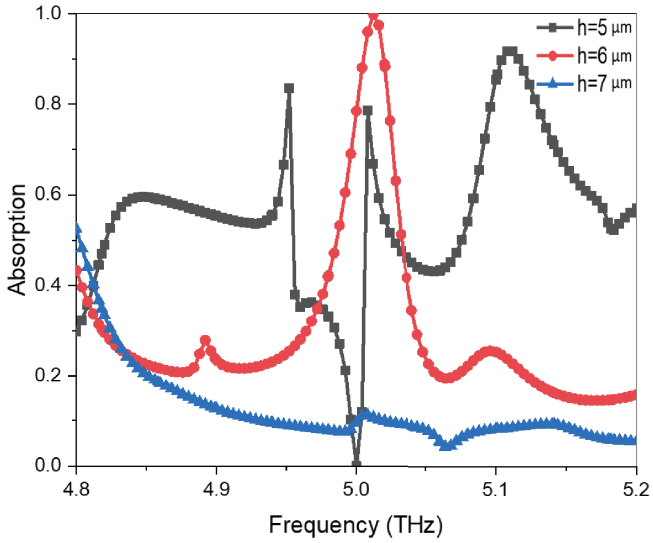

FIGURE 7. Parametric analysis of substrate height.

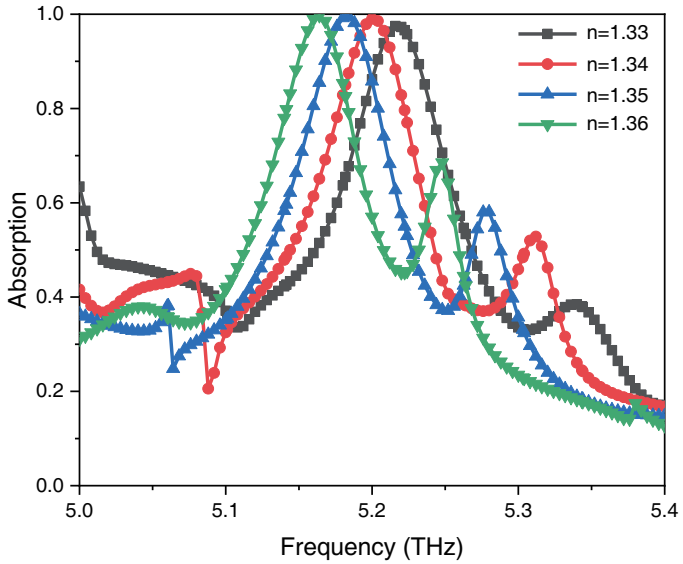

FIGURE 8. Simulation of refractive indices with different alcohol concentrations in water.

For the unit cell dimension, u, and substrate height, h, a parametric sweep is carried out to support the selection of the parameters. The parameter magnitude and resonant frequency are therefore shown to have an inverse relationship. The best absorption and narrowest bandwidth are provided by a unit cell of $u = 120\,\mu$m, which leads to a higher quality factor, according to Figure 6. Figure 7 shows that the optimal peak is obtained when the substrate thickness is $h = 6\,\mu$m. By changing the substrate height, one can achieve a striking reduction in the absorption rate. When the input impedance (around $377\,\Omega$) matches the impedance of empty space (around $377\,\Omega$), the metamaterial absorber achieves its maximum absorption rate. We detect a decrease in the absorption rate as a result of this phenomenon of impedance matching being disturbed by altering the magnitude of the substrate height.

It is possible to acquire the absorption spectra for various refractive index values. For accurate alcohol content in water detection, this observation is crucial. The absorption bands are represented in Figure 8 with a step size of 0.01 for refractive indices which vary from 1.33 to 1.36. The shift in the bands is noteworthy because of the tiny refractive index fluctuation, making it extremely sensitive to the refractive index of the surrounding medium. We also find the absorption rates significantly high for each of the simulated refractive indices values as depicted in Table 2, which further adds to the effectiveness of the proposed sensor.

To construct an RI sensor, the material must be chosen in such a way that the temperature and pressure do not affect the densities so that the refractive index measure is unaffected. Furthermore, it must also be insensitive to the polarization direc-

TABLE 2. Refractive indices of corresponding alcohol percentage in water at room temperature [30] along with the absorptivity rates.

Refractive Index	Resonance Frequency	% of water in Ethanol	% of peak absorption
1.333	5.2271	100	97.45
1.3384	5.2158	90	98.56
1.345	5.2016	80	99.2
1.351	5.1895	70	99.3
1.355	5.1805	60	99.64
1.3578	5.1744	50	99.5
1.3597	5.1725	40	99.75
1.3608	5.1676	30	99.5

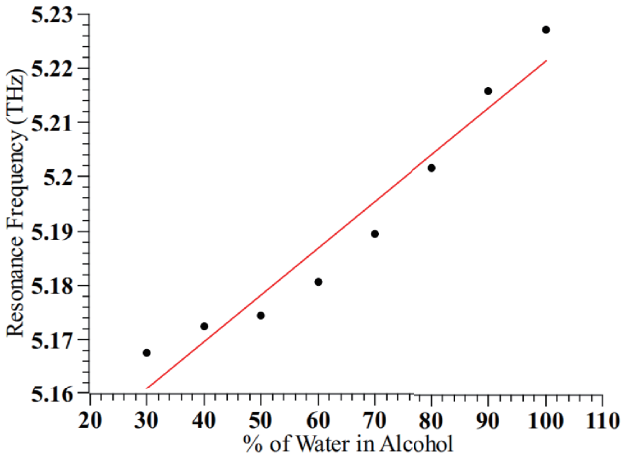

FIGURE 9. Variation in resonace frequency with respect to the percentage of water in alcohol.

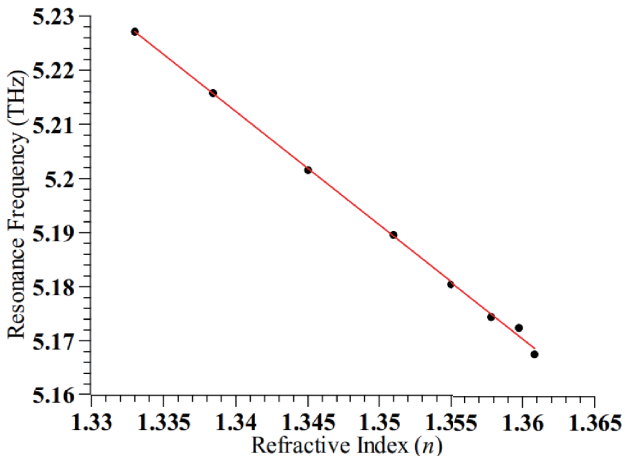

FIGURE 10. Variation in resonance frequency with respect to refractive index corresponding to the % of water in alcohol.

tion. The sensing application removes all barriers to achieve optimal performance by being indifferent to such external influences. Thus in the case of sensing applications, we prefer refractive index sensors for biomedical applications as well as alcohol detection in blood as well as water.

The sensitivity $s = \frac{\Delta f}{\Delta p}$ is the ratio of change in resonance frequency to the change in percentage of water in alcohol solution. Therefore, the sensitivity is determined to be 0.86 GHz per percent addition of water to alcohol, by computing the slope of the resonant frequency vs. refractive index plot in Figure 9. Thus, the linear fit in Figure 9 produces the following equation of straight line where the absolute value of the slope gives the sensitivity of the sensor as follows:

$$f_r = 0.00086p + 5.135 \tag{7}$$

Sensitivity in terms of shift in resonance frequency per unit change in refractive index can also be calculated from Figure 10, and the equation is given in (9).

$$f_r = 8.03 - 2.105n \tag{8}$$

Thus, the sensitivity of the proposed sensor is 2.1 THz/RIU for detecting the contamination of water in alcohol. The corresponding FoM, which is the ratio of the sensitivity to the full-width half-maximum, as given by Eq. (9), is found to be 52.63.

$$FoM = \frac{Sensitivity\,(s)}{FWHM} \tag{9}$$

In [31], the authors simulated how the refractive index of a methanol-ethanol solution would vary as the amount of methanol in the ethanol solution varied. This detection is made feasible by an ultra-sensitive sensor built on dual resonance long-period fiber gratings. This refractive index data is used to detect the % of methanol contamination in alcohol by observing the variation in the resonance frequency. The results are reported in Table 3.

The sensitivity is the ratio of change in resonance frequency to the change in percentage of methanol in alcohol solution. Therefore, the sensitivity is determined to be 0.647 GHz per percent addition of methanol to alcohol, by computing the slope of the resonant frequency vs. refractive index plot in Figure 11. Thus, the linear fit in Figure 11 produces the following equation of straight line where the absolute value of the slope gives the sensitivity of the sensor as follows:

$$f_r = 0.000647p + 5.159 \tag{10}$$

Sensitivity in terms of shift in resonance frequency per unit change in refractive index can also be calculated from Fig-

TABLE 3. Refractive indices of methanol volume percentages in ethanol solution.

Percentage of methanol in ethanol	Refractive index	Frequency (THz)	Absorption rates in %
40	1.3472	5.18182	99.6127
50	1.344	5.192	99.1941
60	1.3407	5.2	98.9399
70	1.3375	5.204	98.7642
80	1.3343	5.212	95.9756
90	1.331	5.216	97.7738
100	1.3278	5.2222	97.089

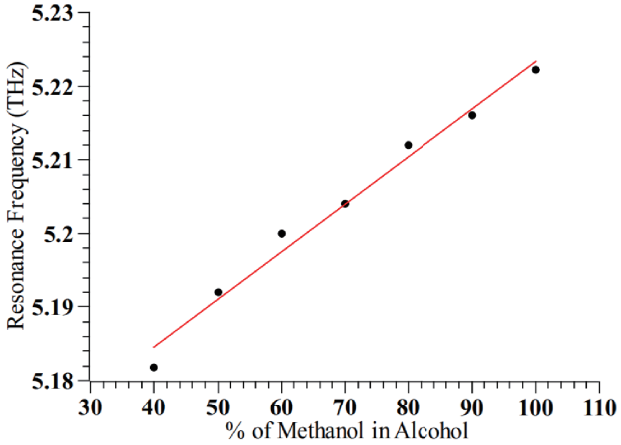

FIGURE 11. Variation in resonace frequency with respect to the percentage of methanol in alcohol.

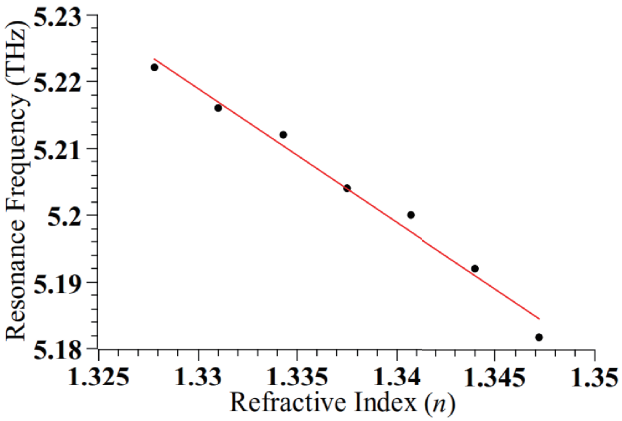

FIGURE 12. Variation in resonance frequency with respect to refractive index corresponding to the % of water in alcohol.

ure 12, and the equation is given in (11).

$$f_r = 7.88 - 1.999n \tag{11}$$

Thus, the sensitivity of the proposed sensor is 1.999 THz/RIU for detecting the contamination of water in alcohol, and the FoM is 49.98.

4. CONCLUSION

Metamaterial absorbers have lately piqued the interest of researchers due to their superior performance as terahertz sensors. The proposed metamaterial contains a triangular patch resonator in the middle surrounded by an array of Strip Resonators followed by an outer square ring. The top and bottom surfaces are made up of gold, and the layer sandwiched in between is an ultra-thin dielectric substrate composed of Gallium Arsenide which provides mechanical flexibility and high TMS sensitivity in a terahertz frequency regime. This design achieves near-perfect absorption of 99.5% at 5.01 THz with a narrow FWHM of 0.04 THz. When the refractive index is changed due to contamination of alcohol with water, the sensitivity is found to be 2.105 THz/RIU, and the FoM is 52.63. Similarly, when the refractive index is changed due to contamination of alcohol with methanol, the sensitivity is found to be 1.999 THz/RIU, and the FoM is 49.98. This sensor is highly sensitive with a higher rate of absorption, and hence it can be used for contamination detection in alcohol. The suggested sensor has the potential to save the lives of adults who consume polluted alcoholic beverages and endanger their lives.

REFERENCES

[1] Ramakrishna, S. A. and T. M. Grzegorczyk, *Physics and Applications of Negative Refractive Index Materials*, CRC Press, 2008.

[2] Bakır, M., M. Karaaslanb, E. Unal, O. Akgol, and C. Sabah, "Microwave metamaterial absorber for sensing applications," *Opto-Electronics Review*, Vol. 25, No. 4, 318–325, 2017.

[3] Appasani, B., P. Prince, R. K. Ranjan, N. Gupta, and V. K. Verma, "A simple multi-band metamaterial absorber with combined polarization sensitive and polarization insensitive characteristics for terahertz applications," *Plasmonics*, Vol. 14, 737–742, 2019.

[4] Cong, L., S. Tan, R. Yahiaoui, F. Yan, W. Zhang, and R. Singh, "Experimental demonstration of ultrasensitive sensing with terahertz metamaterial absorbers: A comparison with the metasurfaces," *Applied Physics Letters*, Vol. 106, No. 3, 031107, 2015.

[5] Srivastava, Y. K., L. Cong, and R. Singh, "Dual-surface flexible THz Fano metasensor," *Applied Physics Letters*, Vol. 111, 201101, 2017.

[6] Gupta, M. and R. Singh, "Terahertz sensing with optimized Q/Veff metasurface cavities," *Advanced Optical Materials*, Vol. 8, No. 16, 1902025, 2020.

[7] Appasani, B., "Temperature tunable seven band terahertz metamaterial absorber using slotted flower–shaped resonator on an InSb substrate," *Plasmonics*, Vol. 16, No. 3, 833–839, 2021.

[8] Mukherjee, P., M. S. Khan, S. Pahadsingh, and B. Appasani, "Terahertz refractive index sensing using metamaterial absorber," in *2022 IEEE 8th World Forum on Internet of Things (WF-IoT)*, 1–5, 2022.

[9] Mohanty, A., O. P. Acharya, B. Appasani, S. K. Mohapatra, and M. S. Khan, "Design of a novel terahertz metamaterial absorber for sensing applications," *IEEE Sensors Journal*, Vol. 21, No. 20, 22 688–22 694, 2021.

[10] Mukherjee, P., S. Pahadsingh, S. Dey, and A. Dasgupta, "Inverted bracket-shaped refractive index sensor with high Q-factor for biomedical applications," in *2022 International Conference on Emerging Trends in Engineering and Medical Sciences (ICETEMS)*, 191–195, 2022.

[11] Nickpay, M.-R., M. Danaie, and A. Shahzadi, "Highly sensitive THz refractive index sensor based on folded split-ring metamaterial graphene resonators," *Plasmonics*, Vol. 17, 237–248, 2021.

[12] Shruti, Sasmita Pahadsingh, and Bhargav Appasani,, "A dual band THz metamaterial based absorber for gas refractive index sensing," in *2022 International Conference on Emerging Trends in Engineering and Medical Sciences (ICETEMS)*, 173–178, 2022.

[13] Banerjee, A., S. Vajandar, and T. Basu, "Prospects in medical applications of terahertz waves," *Terahertz Biomedical and Healthcare Technologies*, 225–239, Elsevier, 2020.

[14] Danciu, M., T. Alexa-Stratulat, C. Stefanescu, G. Dodi, B. I. Tamba, C. T. Mihai, G. D. Stanciu, A. Luca, I. A. Spiridon, L. B. Ungureanu, *et al.*, "Terahertz spectroscopy and imaging: A cutting-edge method for diagnosing digestive cancers," *Materials*, Vol. 12, No. 9, 1519, 2019.

[15] Markelz, A. G. and D. M. Mittleman, "Perspective on terahertz applications in bioscience and biotechnology," *ACS Photonics*, Vol. 9, No. 4, 1117–1126, Apr. 2022.

[16] Gezimati, M. and G. Singh, "Terahertz imaging and sensing for healthcare: Current status and future perspectives," *IEEE Access*, Vol. 11, 18 590–18 619, 2023.

[17] Mittleman, D. M., "Twenty years of terahertz imaging," *Optics Express*, Vol. 26, No. 8, 9417–9431, Apr. 2018.

[18] Banerjee, S., U. Nath, P. Dutta, A. V. Jha, B. Appasani, and N. Bizon, "A theoretical terahertz metamaterial absorber structure with a high quality factor using two circular ring resonators for biomedical sensing," *Inventions*, Vol. 6, No. 4, 78, 2021.

[19] Banerjee, S., P. Dutta, A. V. Jha, B. Appasani, and M. S. Khan, "A biomedical sensor for detection of cancer cells based on terahertz metamaterial absorber," *IEEE Sensors Letters*, Vol. 6, No. 6, 1–4, 2022.

[20] Saadeldin, A. S., M. F. O. Hameed, E. M. A. Elkaramany, and S. S. A. Obayya, "Highly sensitive terahertz metamaterial sensor," *IEEE Sensors Journal*, Vol. 19, No. 18, 7993–7999, 2019.

[21] Xiong, Z., L. Shang, J. Yang, L. Chen, J. Guo, Q. Liu, S. A. Danso, and G. Li, "Terahertz sensor with resonance enhancement based on square split-ring resonators," *IEEE Access*, Vol. 9, 59 211–59 221, 2021.

[22] Rezagholizadeh, E., M. Biabanifard, and S. Borzooei, "Analytical design of tunable THz refractive index sensor for TE and TM modes using graphene disks," *Journal of Physics D: Applied Physics*, Vol. 53, No. 29, 295107, 2020.

[23] Zhang, W., J.-Y. Li, and J. Xie, "High sensitivity refractive index sensor based on metamaterial absorber," *Progress In Electromagnetics Research M*, Vol. 71, 107–115, 2018.

[24] Nickpay, M.-R., M. Danaie, and A. Shahzadi, "Graphene-based tunable quad-band fan-shaped split-ring metamaterial absorber and refractive index sensor for THz spectrum," *Micro and Nanostructures*, Vol. 173, 207473, 2023.

[25] Cheng, Y., Y. Qian, H. Luo, F. Chen, and Z. Cheng, "Terahertz narrowband perfect metasurface absorber based on micro-ring-shaped gaas array for enhanced refractive index sensing," *Physica E: Low-dimensional Systems and Nanostructures*, Vol. 146, 115527, 2023.

[26] Ma, S., P. Zhang, X. Mi, and H. Zhao, "Highly sensitive terahertz sensor based on graphene metamaterial absorber," *Optics Communications*, Vol. 528, 129021, 2023.

[27] Appasani, B., "An octaband temperature tunable terahertz metamaterial absorber using tapered triangular structures," *Progress In Electromagnetics Research Letters*, Vol. 95, 9–16, 2021.

[28] Appasani, B., A. Srinivasulu, and C. Ravariu, "A high Q terahertz metamaterial absorber using concentric elliptical ring resonators for harmful gas sensing applications," *Defence Technology*, Vol. 22, 69–73, 2023.

[29] Mukherjee, P., S. Banerjee, S. Pahadsingh, W. Bhowmik, B. Appasani, and Y. I. Abdulkarim, "Refractive index sensor based on terahertz epsilon negative metamaterial absorber for cancerous cell detection," *Journal of Optoelectronics and Advanced Materials*, Vol. 25, No. 3-4, 128–135, 2023.

[30] Chu, K.-Y. and A. R. Thompson, "Densities and refractive indices of alcohol-water solutions of n-propyl, isopropyl, and methyl alcohols," *Journal of Chemical and Engineering Data*, Vol. 7, No. 3, 358–360, 1962.

[31] Dandapat, K., I. Kumar, and S. M. Tripathi, "Ultrahigh sensitive long-period fiber grating-based sensor for detection of adulterators in biofuel," *Applied Optics*, Vol. 60, No. 24, 7206–7213, 2021.